

# Polycyclic Aromatic Hydrocarbon Biodegradation Rates: A Structure-Based Study

KRISTINE H. WAMMER<sup>†</sup> AND  
CATHERINE A. PETERS\*

Department of Civil and Environmental Engineering,  
Princeton University, Princeton, New Jersey 08544

This study was designed to examine the role of molecular structure in determining the biodegradation rates of polycyclic aromatic hydrocarbons (PAHs). Laboratory experiments were performed in aqueous systems, and data were analyzed in a manner that allowed determination of first-order biodegradation rates independent of bioavailability limitations from physical–chemical processes. An aerobic mixed culture was used, which had been enriched on a broad range of PAHs. The 22 PAHs included in this study ranged in size from two to four rings and included compounds with 5-carbon rings and alkyl substituents. The range of observed biodegradation rates was only 1 order of magnitude, which is much less than that which is typically observed in the field. This supports the findings of other types of studies, which conclude that most of the observed variation in environmental PAH biodegradation rates comes from processes controlling the bioavailability of the compounds and not processes controlling uptake or biotransformation. Rate differences that were observed were attributable either to the presence of a 5-carbon ring or an alkyl substituent in an  $\alpha$  position. Various molecular descriptors that might be expected to correlate with rate-limiting steps in the biodegradation process were used in an attempt to develop a quantitative structure–activity relationship for the PAH biodegradation rates. No significant correlations were found, but rate limitation from interactions with the relevant enzymes remains a possibility.

## Introduction

Polycyclic aromatic hydrocarbons (PAHs) are a class of organic pollutants that are commonly found in the environment, largely due to combustion or processing of hydrocarbon fuels (1–5). Aerobic biodegradation is an important attenuation mechanism for PAHs in the environment (6), so the ability to estimate PAH biodegradation rates is important for predicting environmental fate and for designing remediation efforts. Determining biodegradation rates of PAHs using laboratory experiments can be difficult for two reasons. First, a large number of PAHs are found in the environment, usually as components of very complex mixtures (4, 7–9). Isolating and studying each of these compounds individually would be a substantial task. Second, the solubilities of larger PAHs are orders of magnitude smaller than those of smaller

PAHs. Therefore, larger PAHs, which also tend to be more persistent and more genotoxic (up to about five rings) (10), have solubilities that fall below the detection limits of most analytical techniques. For these reasons, there is a need for the ability to predict the behavior of some PAHs based on the analysis of previously tested compounds. Relationships between molecular structure and biodegradation rate would be extremely useful for this class of compounds.

The majority of PAH biodegradation studies to date have been performed in soils and sediments, either in the laboratory or in the field. In general, an inverse relationship is seen between the molecular weight of the compound and the rate of degradation (11–15). Several studies of PAHs in crude oils have shown similar trends; degradation rates decrease with increasing ring number and increasing number of alkyl substituents and are influenced by the positions of the alkyl substituents (16–20). Physical and chemical processes other than biodegradation, however, affect these observed biodegradation rates. To become available for biodegradation, a compound may need to desorb from sediments or dissolve from a nonaqueous phase liquid. This means that biodegradation rate trends observed in the presence of multiple phases are related not only to the biodegradation of the compound but also to the processes allowing that compound to become bioavailable. Because these bioavailability constraints depend on the physicochemical characteristics of the system, experiments of the type described above cannot be used to find structure–biodegradation relationships that are independent of system parameters. To find such relationships, it is necessary to separate biodegradation from other confounding physical and chemical processes.

A few biodegradation rate studies have been conducted using aqueous systems and thus allow for interpretations that are not confounded by bioavailability constraints (21–24). The findings with regard to the effects of various molecular structure features, however, have been inconsistent. Differences in experimental conditions make comparisons among these studies difficult, and no single data set is comprehensive enough to offer definitive conclusions about structural effects. Another limitation of previous aqueous-system studies of PAH biodegradation rates is that alkyl-substituted PAHs have not been examined as extensively as unsubstituted PAHs despite the fact that they are prevalent in PAH mixtures in the environment (7, 8, 25). Alkylated compounds are especially important when uncombusted fuels are of concern, as in the case of an accidental release of crude oil. For example, of the PAHs found in a sample of *Exxon Valdez* crude oil, 90% were alkylated (26).

In this study, a self-consistent data set of biodegradation rates for a large number of PAHs was developed through laboratory experiments using aqueous systems. The microbial culture used in this study was a consortium of aerobic PAH-degraders enriched on a broad range of PAHs in the lab. The term biodegradation is used here to refer to biologically mediated reactions that result in transformation of a PAH compound rather than reactions that result in mineralization. The PAHs studied ranged in size from two to four rings, including compounds containing 5-carbon rings and compounds with alkyl substituents. This study allowed exploration of relationships between molecular structure characteristics and biodegradation rates in the absence of bioavailability constraints. A variety of descriptors was used to capture molecular structure characteristics and to search for structure–biodegradation rate relationships.

\* Corresponding author phone: (609)258-5645; fax: (609)258-2799; e-mail: cap@princeton.edu.

<sup>†</sup> Present address: Civil Engineering Dept., University of Minnesota, 500 Pillsbury Dr. SE, Minneapolis, MN 55455.

## Experimental Methods

**Chemicals.** PAHs and the surfactant Tween 80 (polyoxyethylenesorbitan monooleate) were purchased from Sigma-Aldrich Corporation (St. Louis, MO) and used without any additional purification. All PAHs were of 98% purity or higher with the following exceptions: anthracene (97%), 1,3-dimethylnaphthalene (96%), indan (95%), 1,4-dimethylnaphthalene (95%), and 1,8-dimethylnaphthalene (95%). Solvents were purchased from Fisher Scientific (Pittsburgh, PA) and were of 99.9% purity. Nutrient buffer pillows were obtained from Hach Company (Loveland, CO) and contained the following nutrients in demineralized water (range of percent by weight): calcium chloride (1.0–5.0%), dibasic potassium phosphate (1.0–5.0%), magnesium sulfate (<5.0%), ferric chloride (<1.0%), monobasic potassium phosphate (<1.0%), sodium phosphate (<1.0%), and ammonium chloride (<1.0%). Water was purified and deionized using HYDRO Service and Supplies Company's Picosystem Plus system (Research Triangle Park, NC).

**PAH Biodegradation Experiments.** Experiments were designed to measure biodegradation rates of PAH substrates in aqueous systems with any potentially rate-limiting physical processes carefully controlled or measured. These experiments were performed individually for each PAH at a concentration significantly below its aqueous solubility to ensure that no separate PAH phase was present. Each experiment involved an "abiotic" and a "biotic" series, each series comprised of between seven and ten 35 mL batch reactors. The abiotic series contained PAH substrate dissolved in an aqueous phase containing necessary trace nutrients at approximately 10–125 ppm (5 nutrient buffer pillows per liter of water), and the biotic series included a 2–3 mL inoculum of a bacterial consortium resulting in a total liquid volume of 27–28 mL.

The bacteria were from an enrichment culture that originated from the Bemidji petroleum spill site in Minnesota (27). The culture was maintained on a mixture of nine PAHs [naphthalene (64 mg/L), 1-methylnaphthalene (16 mg/L), 2-methylnaphthalene (16 mg/L), 2-ethylnaphthalene (16 mg/L), fluorene (9.6 mg/L), phenanthrene (9.6 mg/L), pyrene (0.5 mg/L), fluoranthene (0.4 mg/L), and anthracene (0.2 mg/L)] in our laboratory for several years. The range of molecular features examined in this study (compounds with two to four rings, presence of a 5-carbon ring, presence of an alkyl substituent) was represented by the compounds to which the consortium had been acclimated. No particular molecular feature dominated, so this mixture of compounds would not be expected to preferentially select for organisms able to degrade only a single compound type. The dominant species in the consortium has been identified through 16S RNA gene analysis as *Sphingomonas yanoikuyae* (21 out of 24 colonies on plates) (unpublished study). *Sphingomonas* spp. are ubiquitous geographically, having been isolated even from fuel-contaminated Antarctic soil, and often have broad aromatic hydrocarbon substrate utilization capabilities (28) that are frequently observed among PAH-degrading bacteria (29). The bacteria, which were allowed to grow on the PAH mixture prior to harvesting, were rigorously cleaned with a solution of Tween 80 prior to each experiment to ensure that no residual PAHs were present to affect the rate data. The washing procedure involved several cycles of suspending the bacteria in Tween solution followed by centrifugation. Results demonstrating the effectiveness of this washing procedure, the removal of Tween prior to the experiment, and the lack of sensitivity of the bacteria to Tween 80 at the concentrations used have been published previously (30).

The batch reactors were sealed with butyl-rubber septa to minimize losses through volatilization and were continuously stirred using Teflon stirbars. Dissolved oxygen con-

centration was measured periodically to ensure that aerobic conditions were maintained. The reactors were covered with foil to prevent photochemical reactions. The experiments were performed at  $23 \pm 3$  °C; pH of the solutions in the batch reactors was between 6.9 and 7.3 at the beginning of each experiment. These experiments were similar to others that have been described previously; the reader is referred to this previous work for details omitted here, including PAH solution preparation, bacterial culture maintenance protocol and washing procedure, and method for monitoring dissolved oxygen (21).

PAH substrate concentration (in both the abiotic and biotic reactors) and biomass concentration (in the biotic reactors) were measured over time by sacrificing individual reactor vessels and taking three replicate samples of the aqueous solution. PAH concentrations were measured using a Hewlett-Packard 1050 series high-performance liquid chromatography (HPLC) system equipped with diode-array ultraviolet and fluorescence detectors and a Waters Spherisorb ODS2 column (5  $\mu$ m, 4.0  $\times$  250 mm). The HPLC detection method was unique to each compound; injection volumes, ultraviolet absorbance wavelengths, and fluorescence excitation and emission wavelengths were optimized to maximize sensitivity. Some compounds required more than one method to analyze concentrations that changed over several orders of magnitude through the course of an experiment. Detection limits were 1 order of magnitude below the lowest PAH concentrations analyzed for most experiments; in all experiments the lowest concentration analyzed was at least two times higher than the detection limit. The mobile phase consisted of varying percentages of acetonitrile and water; the flow rate was 1.0 mL/min for each compound.

Samples from the biotic systems were filtered through a 0.2  $\mu$ m Anotop 10 filter (Whatman, Maidstone, England) prior to HPLC analysis to remove biomass material. The filters were pretreated to eliminate sorption concerns. For some of the compounds, sorption to the filter was too significant to eliminate by pretreatment. In these cases, tests were done to determine the fraction lost for each compound, and measured concentrations were corrected using these factors. Throughout the range of the concentrations used in the experiments, it was determined that the fraction lost was a constant for each PAH. The fractions recovered for each PAH were as follows: IND = 0.86, 1MN = 0.87, 2MN = 0.81, 12DMN = 0.88, 14DMN = 0.86, 15DMN = 0.83, 16DMN = 0.68, 26DMN = 0.80, 1EN = 0.79, 2EN = 0.75, ANTH = 0.51, and FLR = 0.81. Unfiltered samples were taken to determine biomass concentration, which was measured by lysing the cells with a sodium hydroxide solution and using a Bradford-type protein assay with bovine serum albumin as the protein standard (Bio-Rad Laboratories, Hercules, CA).

The experiments were performed for a total of 24 PAHs. For two of the most hydrophobic compounds, pyrene and 9-methylanthracene, strong sorption to the Anotop filters made accurate PAH concentration data too difficult to obtain even with correction. This defined the limit for compounds that could be included in this study; reliable measurements would not be obtainable by this method for more strongly sorbing compounds. Table 1 lists the 22 PAHs (with abbreviations) for which successful experiments were performed, the starting PAH substrate and biomass concentration for each experiment, and aqueous solubilities of the compounds (31, 32). Given the range of initial substrate to biomass concentration ratios (0.04–0.2 mg of substrate/mg of protein), the experiments yield extant kinetic parameters per the definitions of Grady et al. (33). Because the experiments were performed over a period of 16 months, it was necessary to ensure that rate differences observed were not due to shifts in the microbial community over time. Therefore, the experiment for naphthalene was performed 4 times,

**TABLE 1. Compounds Studied, Abbreviations Used, Starting Total PAH Concentrations, Biomass Concentrations, and Aqueous Solubilities**

compound	abbreviation	$C_0$ (mg/L)	$X$ (mg of protein/L)	aq solubility (mg/L)
indan	IND	0.093	2.25	100
indene	INDE	0.12	1.35	332
naphthalene (1)	NPH	0.20	1.04	31
naphthalene (2)	NPH	0.13	1.32	31
naphthalene (3)	NPH	0.14	1.86	31
naphthalene (4)	NPH	0.09	1.56	31
1-methylnaphthalene	1MN	0.28	1.25	28
2-methylnaphthalene	2MN	0.25	1.44	25
1,2-dimethylnaphthalene	12DMN	0.082	1.72	14.9
1,3-dimethylnaphthalene	13DMN	0.14	1.25	8
1,4-dimethylnaphthalene	14DMN	0.074	1.63	11.4
1,5-dimethylnaphthalene	15DMN	0.078	2.20	3.1
1,6-dimethylnaphthalene	16DMN	0.068	1.90	0.9
1,8-dimethylnaphthalene	18DMN	0.10	1.71	12.9
2,6-dimethylnaphthalene (1)	26DMN	0.057	1.07	1.7
2,6-dimethylnaphthalene (2)	26DMN	0.094	1.82	1.7
2,7-dimethylnaphthalene	27DMN	0.064	2.24	14.9
2,3,5-trimethylnaphthalene	235TMN	0.074	1.22	4.8
1-ethylnaphthalene	1EN	0.085	1.60	10.1
2-ethylnaphthalene	2EN	0.17	1.62	8
acenaphthene	ACE	0.071	1.43	3.8
phenanthrene	PHN	0.10	1.30	1.1
anthracene	ANTH	0.035	1.94	0.05
fluorene	FLR	0.27	1.42	1.9
1-methylfluorene	1MFLR	0.083	1.69	1.1
fluoranthene	FLN	0.096	1.78	0.26

including at the beginning and end of the 16 month time period. The experiment for 2,6-dimethylnaphthalene was also performed twice with 8 months between repeats.

**Model Equations.** A model was developed to describe the processes controlling PAH concentration in the experimental systems. The purpose of the model was to interpret experimental data, thus allowing estimation of biodegradation rate parameters. The experiments were performed with sufficiently high initial biomass concentrations such that changes in biomass concentration were negligible. Therefore, no biomass growth equations are included.

PAH substrates were considered to be dissolved in the aqueous phase, partitioned to the experimental apparatus or headspace, or sorbed to the biomass. A mass balance for PAH in the experimental systems can therefore be written as:

$$M_T = M + M_{app} + M_{bio} \quad (1)$$

where  $M_T$  is total mass of PAH present at any given point in time,  $M$  is mass of PAH in the aqueous phase,  $M_{app}$  represents the mass of PAH sorbed to the apparatus and present in the reactor headspace, and  $M_{bio}$  is mass of PAH sorbed to the biomass. Dividing each of these masses by the volume of the aqueous phase, we obtain an equation in terms of effective concentrations (mg/L):

$$C_T = C + C_{app} + C_{bio} \quad (2)$$

Partitioning was found to be fast relative to biodegradation kinetics, so partitioning processes were assumed to be instantaneous. The relationship between the effective concentration of PAH partitioned to the apparatus/headspace and the dissolved PAH concentration is linearly modeled as:

$$C_{app} = K_a C \quad (3)$$

where  $K_a$  (–) is referred to as the abiotic partitioning coefficient. The effective concentration of PAH sorbed to the

biomass is linearly related to the dissolved PAH concentration as:

$$C_{bio} = K_b X C \quad (4)$$

where  $K_b$  is the biotic partitioning coefficient ((mg of protein/L)<sup>-1</sup>) and  $X$  is the biomass concentration (mg of protein/L). It should be noted that  $X$  is the total biomass population, which may include some fraction of inactive biomass.

The differential form of the mass balance equation is written to mathematically separate rate changes due to biodegradation of the substrate and rate changes due to abiotic processes, which may have included slow volatilization to the headspace and/or sorption to components of the reaction vessel. We observed that losses over time in the abiotic experiments were first order for all PAHs. The data from the abiotic experiments were therefore used to estimate an abiotic first-order loss coefficient,  $k_a$  (h<sup>-1</sup>). The initial PAH substrate concentrations were designed to be sufficiently low such that substrate biodegradation kinetics were also first order. Available literature data of Michaelis–Menten affinity constants for a subset of the compounds studied here (NPH, 1MN, and PHN) were used as a guide (21, 23, 24, 34), and the experimental observations for all the compounds were checked to validate this assumption. The overall governing equation is therefore

$$\frac{dC_T}{dt} = (1 + K_a + K_b X) \frac{dC}{dt} = -k_b X C - k_a C \quad (5)$$

where  $k_b$  [(mg of protein/L)<sup>-1</sup> (h)<sup>-1</sup>] is defined as the biomass-normalized first-order rate coefficient. This is the biodegradation rate parameter that is compared for the PAHs studied here. This parameter represents the rate of biodegradation of dissolved PAH. It is not confounded by any physical–chemical processes, and it is independent of the biomass concentration, which was slightly different for each PAH experiment.

**Data Interpretation.** Figure 1a shows PAH concentration as a function of time for the indene (INDE) experiment and allows illustration of how the model parameters were obtained. Note that when depicted on a log scale the linearity of the concentration measurements indicates that first-order substrate depletion occurred in both the abiotic and the biotic series after the initial rapid partitioning processes. This log-linearity was also found for the other PAHs studied. This suggests that the kinetic models used in eq 5 are appropriate for interpreting data from these experiments. Figure 1b shows the biomass concentration measurements for the INDE experiment; as stated previously, changes in biomass concentrations during each of the experiments were not statistically significant. The abiotic partitioning coefficient  $K_a$  was estimated using the measured total initial substrate concentration  $C_{T,0}$  and the aqueous phase initial substrate concentration in the abiotic system  $C_{a,0}$ :

$$K_a = \frac{C_{T,0} - C_{a,0}}{C_{a,0}} \quad (6)$$

$C_{a,0}$  was determined by performing a linear regression for the abiotic data and finding the point at which that line intersected the  $y$ -axis. This regression is not shown on the figure so the data are not obscured, but  $C_{a,0}$  is indicated. The biotic partitioning coefficient  $K_b$  was estimated using  $C_{T,0}$  and the aqueous phase initial substrate concentration in the biotic system,  $C_{b,0}$ :

$$K_b = \frac{1}{X} \left( \frac{C_{T,0} - K_a C_{b,0} - C_{b,0}}{C_{b,0}} \right) \quad (7)$$

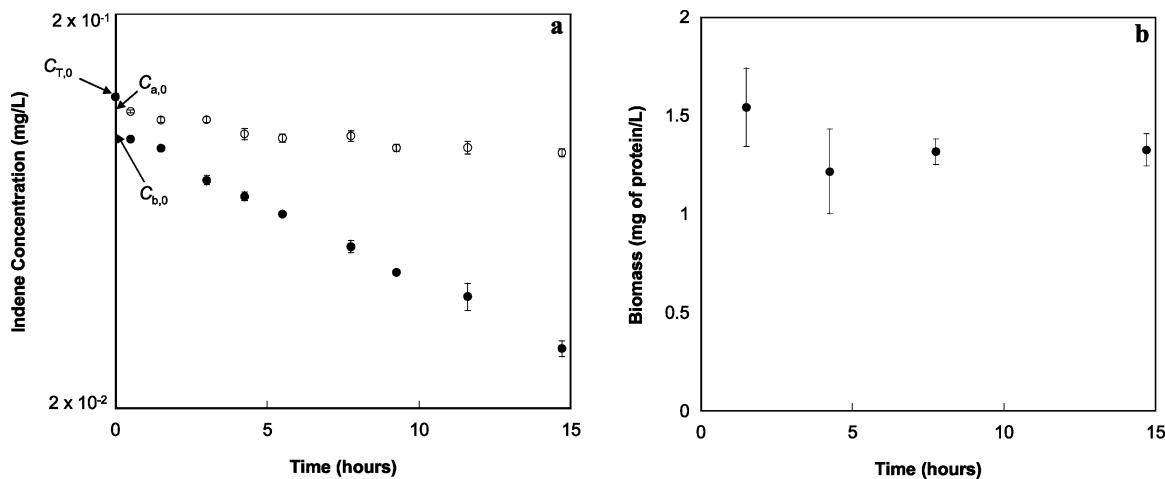


**FIGURE 1.** Substrate concentration data (a) and biomass data (b) from the abiotic (○) and biotic (●) series of the indene (INDE) biodegradation experiment. Error bars represent one standard error. Total starting PAH concentration ( $C_{T,0}$ ), and inferred values of initial aqueous phase concentrations in the abiotic ( $C_{a,0}$ ) and biotic ( $C_{b,0}$ ) systems are indicated.

The value of  $C_{b,0}$  was determined by the same method as  $C_{a,0}$  using the biotic data. The abiotic decay coefficient  $k_a$  was estimated by fitting the following equation to the abiotic system data:

$$(1 + K_a) \frac{dC}{dt} = -k_a C \quad (8)$$

The biomass-normalized first-order rate coefficient  $k_b$  was estimated by fitting eq 5 to the biotic substrate concentration data using the independently estimated parameters ( $k_a$ ,  $K_a$ , and  $K_b$ ) and the initial substrate concentration  $C_{b,0}$ . The integrated form of eq 5 was used, allowing the data to be fit using linear regression. The number of concentration data points used to fit  $k_a$  and  $k_b$  ranged from 6 to 9.

**Molecular Descriptors.** The topological descriptors of molecular structure that were used in this study were the molecular connectivity descriptors of Kier and Hall (35). These were calculated using the program Graph III (36). Other molecular descriptors were calculated using the software packages PC Spartan Pro (Wavefunction, Inc., Irvine, CA) and CAChe ProjectLeader (Fujitsu, Ltd., Beaverton, OR). Equilibrium geometries, total and molecular orbital energies, and charge distributions were calculated at a Hartree–Fock level of theory, using the 3-21G<sup>(\*)</sup> basis set. Polarizability, superdelocalizability, and heats of formation were calculated at a semiempirical level, using MOPAC 2000. Molar refractivity and  $\log K_{ow}$  were calculated in CAChe using atomic parameters developed by Ghose et al. (37). Diffusivity was calculated using an empirical equation developed for PAHs in aqueous systems (38).

## Results and Discussion

**Experimental Results.** Other than  $k_b$ , values of the estimated parameters are not reported here, but they generally followed expected trends (e.g., volatile PAHs had higher values of  $k_a$ , and hydrophobic PAHs had higher values of  $K_b$ ). Values of  $k_b$  for the 22 PAHs are listed in Table 2 and illustrated in Figure 2. The standard errors shown in Table 2 (depicted as error bars in Figure 2) were determined by propagating errors associated with the various parameters and variables through the model; the standard errors ranged from 11 to 61% (39). The largest contributions to the errors in  $k_b$  came from variability in the biomass concentration measurements.

The  $k_b$  values reported for NPH and 26DMN represent averages of the multiple experiments performed. It was determined that the errors in the data were log-normally

distributed (39); therefore, a geometric mean rather than an arithmetic mean was taken, and the errors of the natural logs of the values were averaged to give fair weight to each estimate. The geometric means were calculated as  $[(0.36)(0.16)(0.13)(0.27)]^{1/4} = 0.21$  (mg of protein/L)<sup>-1</sup> (h)<sup>-1</sup> for NPH and  $[(0.21)(0.19)]^{1/2} = 0.20$  (mg of protein/L)<sup>-1</sup> (h)<sup>-1</sup> for 26DMN. The standard errors associated with these means were estimated using the pooled standard errors of the natural logs of the individual estimates. The resulting standard errors were 0.04 for NPH and 0.05 for 26DMN. The details of this analysis can be found elsewhere (39). The value of  $k_b$  that was estimated for each the four naphthalene experiments did not follow any trend over time, and the pooled standard errors for NPH and 26DMN were comparable to the standard errors estimated for other compounds. This supports our assumption that differences in the estimated biodegradation rates for different compounds are not due to changes in the bacterial consortium over time.

**Relationships between Biodegradation Rates and Molecular Structure Characteristics.** The PAHs in this study can be divided into two types: PAHs comprised of only fused six-carbon benzenoid rings are known as alternant PAHs, and PAHs containing other types of rings are known as nonalternant PAHs. PAH structures are also characterized by substituent positions. Figure 3 uses NPH to illustrate the general system used to designate positions on a ring (40).

As mentioned in the Introduction, previous work to correlate PAH biodegradation rates in aqueous systems with structural features has been inconclusive. Two common findings, however, have been that alkyl groups and 5-carbon rings are likely to be important in such correlations. Aitken et al. (24) studied degradation of a range of PAHs by several organisms. Examination of the specific oxygen uptake rates reported in the study reveals that, while rate patterns varied for the different isolates, in most cases alternant PAHs were degraded more rapidly than nonalternant PAHs. Methylation of naphthalene usually decreased biodegradation rate, with 1-methylnaphthalene (alkyl group in an  $\alpha$  position) degrading more slowly than 2-methylnaphthalene (alkyl group in a  $\beta$  position). LeBlond et al. (22) performed experiments involving mixtures of PAHs and found that increasing the number of alkyl substituents and the size of substituents slowed transformation rates. Knightes and Peters (21) examined 10 PAHs individually in aqueous phase experiments. They concluded that alkylation appeared to significantly affect PAH biodegradation and that nonalternant PAHs biodegraded

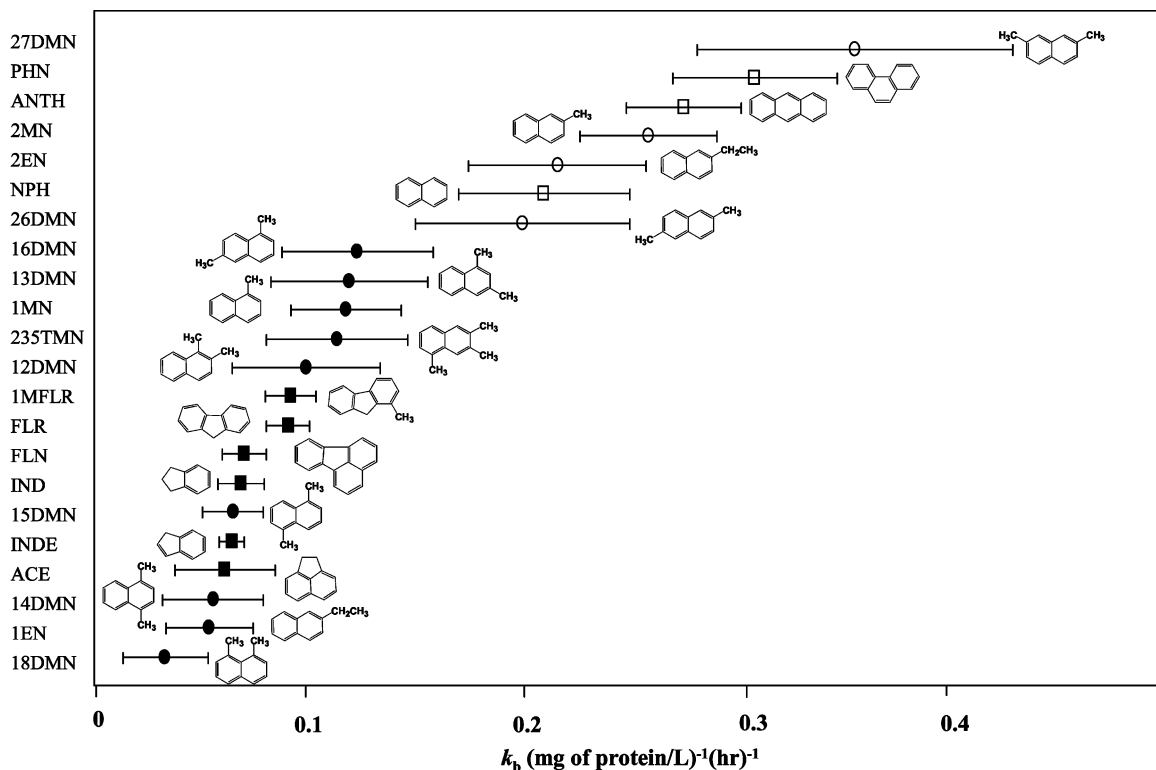


FIGURE 2. Biomass-normalized first-order rate coefficients for all 22 PAHs studied. Error bars represent one standard error. Different symbols are used to represent alternant PAHs with no substituents ( $\square$ ), with  $\beta$  substituents only ( $\circ$ ), with  $\alpha$  substituents ( $\bullet$ ), and nonalternant PAHs ( $\blacksquare$ ).

TABLE 2. First-Order Biomass-Normalized Rate Coefficients ( $k_b$ ) and Values of Selected Molecular Descriptors<sup>a</sup>

compound	$k_b$ ((mg of protein/L) <sup>-1</sup> (h) <sup>-1</sup> )	log $K_{ow}$ (-)	HOMO energy (eV)	total energy (10 <sup>5</sup> kcal/mol)	first-order valence connectivity index $^1X^*(-)$	polarizability (-)	molecular volume (Å <sup>3</sup> )	diffusivity (10 <sup>-6</sup> cm <sup>2</sup> /s)
27DMN	0.36 ± 0.07	3.983	-7.82	-2.88	4.23	15.26	198.68	5.0
PHN	0.31 ± 0.04	4.051	-7.86	-3.34	4.82	18.31	210.26	4.8
ANTH	0.28 ± 0.03	4.051	-7.16	-3.34	4.81	19.46	211.14	4.9
2MN	0.26 ± 0.03	3.516	-7.89	-2.64	3.82	13.84	178.33	5.9
2EN	0.22 ± 0.04	3.912	-7.87	-2.88	4.38	14.95	198.8	6.5
NPH	0.21 ± 0.04	3.049	-7.98	-2.39	3.41	12.42	157.99	7.1
26DMN	0.20 ± 0.05	3.983	-7.78	-2.88	4.23	15.29	198.68	5.0
16DMN	0.12 ± 0.04	3.983	-7.77	-2.88	4.23	15.10	198.07	6.6
13DMN	0.12 ± 0.04	3.983	-7.76	-2.88	4.23	15.09	198.06	6.4
1MN	0.12 ± 0.03	3.516	-7.85	-2.64	3.82	13.68	177.7	7.5
235TMN	0.11 ± 0.03	4.450	-7.68	-3.12	4.65	16.46	217.79	4.4
12DMN	0.10 ± 0.03	3.983	-7.73	-2.88	4.24	15.03	197.24	6.7
1MFLR	0.092 ± 0.01	4.232	-7.89	-3.35	5.03	17.35	219.30	4.5
FLR	0.091 ± 0.01	3.765	-7.93	-3.11	4.61	16.13	199.17	5.2
FLN	0.070 ± 0.01	4.371	-7.87	-3.82	5.57	21.26	231.92	4.3
IND	0.068 ± 0.01	2.873	-8.64	-2.16	3.53	10.06	152.68	9.1
15DMN	0.065 ± 0.01	3.983	-7.73	-2.88	4.24	14.96	197.34	5.0
INDE	0.064 ± 0.01	2.613	-8.12	-2.16	3.21	10.59	146.35	9.7
ACE	0.061 ± 0.02	3.479	-7.64	-2.87	4.45	14.59	185.46	5.8
14DMN	0.055 ± 0.02	3.983	-7.71	-2.88	4.24	14.99	197.38	6.7
1EN	0.054 ± 0.02	3.912	-7.84	-2.88	4.38	14.72	197.51	6.7
18DMN	0.033 ± 0.02	3.983	-7.65	-2.88	4.24	14.98	196.46	5.0
$R^2$		.009	0.03	0.01	0.0002	0.04	0.008	0.05

<sup>a</sup> Errors listed for  $k_b$  are one standard error. Reported  $R^2$  from regression with natural log of  $k_b$ .

more slowly than alternant PAHs of similar molecular size. The presence and position of alkyl substituents has also been reported to affect aqueous phase biodegradation rates in several studies involving monocyclic aromatic compounds (41–44). However, for monocyclic compounds it is not possible to define  $\alpha$  and  $\beta$  positions so the relevance of those observations in this context is limited.

Examination of the data in Figure 2 shows that some of the molecular characteristics that have been suggested to influence biodegradation rate in other studies in fact had no effect in the current study. The number of substituents present does not appear to affect biodegradation rate; 1-methylnaphthalene, 1,3-dimethylnaphthalene, and 2,3,5-trimethylnaphthalene are all biodegraded at the same rate.

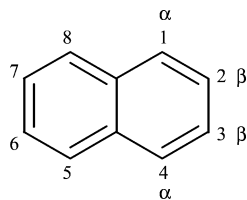


**FIGURE 3.** System used for naming positions on the rings of naphthalene (figure adapted from ref 40).

The presence of an alkyl substituent and substituent length also are not necessarily important, as can be seen by comparing the  $k_b$  values of naphthalene, 2-methylnaphthalene, and 2-ethylnaphthalene.

In this study, just two specific structural features were found to influence biodegradation rates: the presence of a substituent in an  $\alpha$  position and the presence of a 5-carbon ring. Different symbols have been applied to the data in Figure 2 to help illustrate this finding. All alternant compounds with no substituents or only  $\beta$  substituents were found to be biodegraded faster than the other compounds included in the study. All nonalternant compounds, from indene to 1-methylfluorene, were found to be degraded at approximately the same rate and degraded more slowly than the two groups of compounds mentioned previously. Alternant compounds that contain at least one substituent in an  $\alpha$  position, like the nonalternant compounds, degraded more slowly than the alternant PAHs that are unsubstituted or have  $\beta$  substituents only. Furthermore, compounds with one  $\alpha$  substituent degraded at essentially the same rate, and compounds with two  $\alpha$  substituents (15DMN, 14DMN, and 18DMN) were some of the most slowly degrading compounds in this study. Therefore, we conclude that both a nonalternant ring structure and  $\alpha$  alkylation significantly decrease biodegradation rate.

The findings from this study do support findings previously reported in the literature in regard to the role of bioavailability constraints. Knights and Peters (21) found that biodegradation rates measured in aqueous systems did not correlate with hydrophobicity metrics as is usually seen in sediment/water systems. This suggests that the physical and chemical processes governing bioavailability play the most important role in determining rates in the field. The present study supports the hypothesis that much of the variation in observed biodegradation rates in the environment is due to processes other than biodegradation itself. In the environment, biodegradation rates of PAHs of sizes comparable to those studied here can range over several orders of magnitude. For the 22 compounds studied here, the variation in rate coefficients is just 1 order of magnitude. In addition, the inverse relationship between compound size and biodegradation rate usually observed in soils and sediments was not observed here. Statistically insignificant rate differences were observed, for example, among fluoranthene (four rings), acenaphthene (three rings), and indan (two rings), suggesting no relationship between the size of the compound and the rate. Similarly, the differences among naphthalene (two rings), phenanthrene (three rings), and anthracene (three rings) are not statistically significant. Therefore, these previously reported relationships, observed in multiphase systems, are likely due to differences in the bioavailability of the compounds rather than relative biodegradation rates.

#### Quantitative Structure–Biodegradation Relationships.

The possibility of developing a quantitative structure–activity relationship (QSAR) to describe correlations between molecular structure features and biodegradation rates of PAHs was assessed. The first objective was to determine whether correlating the measured biodegradation rates with ap-

propriate molecular descriptors would allow development of a predictive equation. The second objective was to gain mechanistic insight into potential rate-limiting steps in the biodegradation process based on the strength of correlation with different types of molecular descriptors.

Table 2 lists the 22 PAHs for which  $k_b$  values were estimated (listed in descending order of biodegradation rate) along with estimated values of selected molecular descriptors. Examination of the table and the reported  $R^2$  values reveals no significant correlations between rate and any of the descriptors listed for the two- to four-ring PAHs included in the study. Table 2 includes a representative set of descriptors rather than all descriptors examined, but no significant correlations were seen with any of the descriptors chosen in this study. Although  $R^2$  values are reported only for univariate regressions here, no significant predictive power was seen for any combinations of the reported variables in two- and three-variable multivariate regressions. We acknowledge that our study did not include an exhaustive analysis of all possible molecular descriptors including many types of topological and topographic descriptors, but those that were included hold the greatest promise in providing mechanistic insight. If a predictive QSAR equation was the only goal, it may be possible to generate one using topological or other descriptors.

The descriptors included in the table represent types of descriptors that may be expected to correlate with various steps of the biodegradation reaction (45). In the first steps of the biodegradation process, the PAH substrate must enter the bacterial cell by crossing the cell wall and membrane and then diffuse through the cell cytoplasm to reach the enzyme that will initiate the biodegradation reaction. It has been shown that for at least some PAH-degrading bacteria the uptake of PAHs into the cell occurs via passive partitioning and diffusion processes (46). Active transport mechanisms are involved only in PAH efflux and do not have significant effects on degradation rate. Because uptake via passive transport tends to correlate with descriptors that capture hydrophobicity of the compound, such as  $\log K_{ow}$  and polarizability (45), the lack of relationship between biodegradation rates and these descriptors makes it unlikely that crossing into the cell is an important rate-determining step. Likewise, lack of correlation with the diffusivity of the PAHs suggests that diffusion through the cytoplasm is unlikely to be an important step.

In some environmental systems, the next steps in the biodegradation process would be those associated with enzyme induction. In this system, it is assumed that enzyme induction has already occurred due to prior exposure to PAHs. The remaining steps in the biodegradation process involve binding to the initial metabolic enzyme and the chemical transformation mediated by that enzyme. Biologically mediated chemical transformation of PAH compounds has been shown to proceed through addition of molecular oxygen to one of the aromatic rings by a dioxygenase enzyme (47). If chemical transformation is rate limiting, it is reasonable to anticipate a correlation with a descriptor that contains information about the susceptibility of a PAH to electrophilic attack. No such correlation is seen with the energy of the highest occupied molecular orbital (HOMO), which is an indicator of how much energy is required to remove an electron from the molecule. Not only is there a lack of correlation, but also the HOMO energies of the 22 PAHs are nearly identical, which makes it unlikely that this molecular feature would have any predictive power, even with a larger data set. It is more difficult to assign one type of descriptor that should correlate with the step of binding to the enzyme because hydrophobic, steric, and electronic effects could all be important. However, we might expect correlation with a descriptor that contains information about compound size

and shape if fitting into the active site of the enzyme is important. Two descriptors in Table 2, molecular volume and the first-order valence connectivity index, are general size and shape descriptors. The lack of correlation with these descriptors suggests that, even if binding with the enzyme is a rate-limiting step, the size of the PAH is not important at least within the range of compounds examined here.

From this analysis, we cannot rule out the possibility that enzyme-binding and/or chemical transformation are the rate-limiting steps. Because we saw no relationships with descriptors expected to correlate with the first steps of the biodegradation process, we hypothesize that the rate-limiting steps are indeed most likely those involving interactions with the relevant enzymes and that information about the PAHs in the context of these interactions would need to be examined to understand what causes the observed rate differences. For example, comparing 1MN and 2MN in Table 2 reveals no obvious descriptors that can adequately distinguish between PAHs with substituents in the  $\alpha$  or  $\beta$  position. However, once a PAH is bound to the enzyme, this structural difference may significantly impact the rate at which the chemical transformation occurs. Perhaps a substituent in an  $\alpha$  position interferes sterically with active site residues. Similarly, the structural differences between alternant and nonalternant PAHs (e.g., fluorene and phenanthrene) are not significant enough to cause markedly different values in traditional molecular descriptors. However, it may be the case that a slightly nonplanar 5-carbon ring makes fitting into a narrow enzyme binding pocket more difficult. Kinetic and thermodynamic factors specific to the enzyme-mediated reaction may also be important in explaining observed differences in biodegradation rates, as may binding energies.

In summary, we have shown that, for the PAHs included in this study and for the enrichment culture in our lab, the only structural features that result in a slower biodegradation rate are the presence of a 5-carbon ring or a substituent in an  $\alpha$  position. This information allows prediction of relative biodegradation rates based on structure but could not be captured for use in a QSAR using molecular descriptors that might be expected to correlate with potential rate-limiting steps in the biodegradation process. This lack of correlation, however, does not rule out the possibility that the rate-limiting steps are those involving the enzyme or enzymes. In addition, this study supports a growing body of evidence that biodegradation rates for a broad range of PAHs are quite similar once bioavailability constraints have been removed. It also supports the idea that relationships between observed biodegradation rates in some environmental systems and properties such as molecular weight and hydrophobicity are most likely due to bioavailability constraints and do not reflect biodegradation rate trends.

## Acknowledgments

This study was supported by the United States Environmental Protection Agency (STAR fellowship U915553), the National Science Foundation (Grant EAR-9708406), and the American Association of University Women.

## Literature Cited

- Lopes, T. J.; Furlong, E. T. Occurrence and potential adverse effects of semivolatile organic compounds in streambed sediment, United States, 1992–1995. *Environ. Toxicol. Chem.* **2001**, *20*, 727–737.
- Miles, C. J.; Delfino, J. J. Priority pollutant polycyclic aromatic hydrocarbons in Florida sediments. *Bull. Environ. Contam. Toxicol.* **1999**, *63*, 226–234.
- Luthy, R. G.; Dzombak, D. A.; Peters, C. A.; Roy, S. B.; Ramaswami, A.; Nakles, D. V.; Nott, B. R. Remediating tar-contaminated soils at manufactured-gas plant sites. *Environ. Sci. Technol.* **1994**, *28*, 266A–276A.

- Hites, R. A.; Laflamme, R. E.; Windsor, J. G., Jr. In *Petroleum in the Marine Environment*; Petrakis, L., Weiss, F. T., Eds.; American Chemical Society: Washington, DC, 1980; Vol. 185, pp 289–311.
- Laflamme, R. E.; Hites, R. A. The global distribution of polycyclic aromatic hydrocarbons in recent sediment. *Geochim. Cosmochim. Acta* **1978**, *42*, 289–303.
- Cerniglia, C. E. Biodegradation of polycyclic aromatic hydrocarbons. *Curr. Opin. Biotechnol.* **1993**, *4*, 331–338.
- Burkhard, L. P.; Sheedy, B. R. Evaluation of screening procedures for bioconcentratable organic chemicals in effluents and sediments. *Environ. Toxicol. Chem.* **1995**, *14*, 697–711.
- Peters, C. A.; Luthy, R. G. Coal-tar dissolution in water-miscible solvents – experimental evaluation. *Environ. Sci. Technol.* **1993**, *27*, 2831–2843.
- Yu, X. B.; Wang, X. P.; Bartha, R.; Rosen, J. D. Supercritical fluid extraction of coal-tar contaminated soil. *Environ. Sci. Technol.* **1990**, *24*, 1732–1738.
- Cerniglia, C. E. Biodegradation of polycyclic aromatic hydrocarbons. *Biodegradation* **1992**, *3*, 351–368.
- Park, K. S.; Sims, R. C.; Dupont, R. R.; Doucette, W. J.; Matthews, J. E. Fate of PAH compounds in 2 soil types—influence of volatilization, abiotic loss and biological activity. *Environ. Toxicol. Chem.* **1990**, *9*, 187–195.
- Heitkamp, M. A.; Cerniglia, C. E. Effects of chemical structure and exposure on the microbial degradation of polycyclic aromatic hydrocarbons in fresh-water and estuarine ecosystems. *Environ. Toxicol. Chem.* **1987**, *6*, 535–546.
- Bossert, I. D.; Bartha, R. Structure–biodegradability relationships of polycyclic aromatic hydrocarbons in soil. *Bull. Environ. Contam. Toxicol.* **1986**, *37*, 490–495.
- Herbes, S. E. Rates of microbial transformation of polycyclic aromatic hydrocarbons in water and sediments in the vicinity of a coal-coking waste-water discharge. *Appl. Environ. Microbiol.* **1981**, *41*, 20–28.
- Herbes, S. E.; Schwall, L. R. Microbial transformation of polycyclic aromatic hydrocarbons in pristine and petroleum-contaminated sediments. *Appl. Environ. Microbiol.* **1978**, *35*, 306–316.
- Bastow, T. P.; van Aarssen, B. G. K.; Alexander, R.; Kagi, R. I. Biodegradation of aromatic land-plant biomarkers in some Australian crude oils. *Org. Geochem.* **1999**, *30*, 1229–1239.
- Fisher, S. J.; Alexander, R.; Kagi, R. I.; Oliver, G. A. In *Western Australian Basins Symposium*, Perth, Western Australia, 1998; pp 185–194.
- Bayona, J. M.; Albaiges, J.; Solanas, A. M.; Pares, R.; Garrigues, P.; Ewald, M. Selective aerobic degradation of methyl-substituted polycyclic aromatic hydrocarbons in petroleum by pure microbial cultures. *Int. J. Environ. Anal. Chem.* **1986**, *23*, 289–303.
- Solanas, A. M.; Pares, R.; Bayona, J. M.; Albaiges, J. Degradation of aromatic petroleum hydrocarbons by pure microbial cultures. *Chemosphere* **1984**, *13*, 593–601.
- Volkman, J. K.; Alexander, R.; Kagi, R. I.; Rowland, S. J.; Sheppard, P. N. Biodegradation of aromatic hydrocarbons in crude oils from the barrow sub-basin of western Australia. *Org. Geochem.* **1984**, *6*, 619–632.
- Knightes, C. D.; Peters, C. A. Aqueous phase biodegradation kinetics of ten PAHs. *Environ. Eng. Sci.* **2003**, *20*, 207–218.
- LeBlond, J. D.; Schultz, T. W.; Sayler, G. S. Observations on the preferential biodegradation of selected components of polycyclic aromatic hydrocarbon mixtures. *Chemosphere* **2001**, *42*, 333–343.
- Guha, S.; Peters, C. A.; Jaffe, P. R. Multisubstrate biodegradation kinetics of naphthalene, phenanthrene, and pyrene mixtures. *Biotechnol. Bioeng.* **1999**, *65*, 491–499.
- Aitken, M. D.; Stringfellow, W. T.; Nagel, R. D.; Kazunga, C.; Chen, S. H. Characteristics of phenanthrene-degrading bacteria isolated from soils contaminated with polycyclic aromatic hydrocarbons. *Can. J. Microbiol.* **1998**, *44*, 743–752.
- Garcia, K. L.; Delfino, J. J.; Powell, D. H. Non-regulated organic compounds in Florida sediments. *Water Res.* **1993**, *27*, 1601–1613.
- Stubblefield, W. A.; Hancock, G. A.; Ford, W. H.; Ringer, R. K. Acute and subchronic toxicity of naturally weathered Exxon Valdez crude oil in mallards and ferrets. *Environ. Toxicol. Chem.* **1995**, *14*, 1941–1950.
- Jahan, K.; Ahmed, T.; Maier, W. J. Factors affecting the nonionic surfactant-enhanced biodegradation of phenanthrene. *Water Environ. Res.* **1997**, *69*, 317–325.

- (28) Baraniecki, C. A.; Aislabie, J.; Foght, J. M. Characterization of *Sphingomonas* sp. Ant 17, an aromatic hydrocarbon-degrading bacterium isolated from Antarctic soil. *Microb. Ecol.* **2002**, *43*, 44–54.
- (29) Chen, S. H.; Aitken, M. D. Salicylate stimulates the degradation of high molecular weight polycyclic aromatic hydrocarbons by *Pseudomonas saccharophila* P15. *Environ. Sci. Technol.* **1999**, *33*, 435–439.
- (30) Knightes, C. D. Ph.D. Thesis, Princeton University, Princeton, NJ, 2000.
- (31) Syracuse Research Corporation. *PHYSPROP Database*; <http://www.syrres.com/esc/physdemo.htm>.
- (32) Mackay, D.; Shui, W. Y.; Ma, K. C. *Illustrated Handbook of Physical–Chemical Properties and Environmental Fate of Organic Chemicals*; Lewis Publishers: Chelsea, MI, 1992.
- (33) Grady, C. P. L., Jr.; Smets, B. F.; Barbeau, D. S. Variability in kinetic parameter estimates: A review of possible causes and a proposed terminology. *Water Res.* **1996**, *30*, 742–748.
- (34) Stringfellow, W. T.; Aitken, M. D. Comparative physiology of phenanthrene degradation by 2 dissimilar *Pseudomonas* isolated from a creosote-contaminated soil. *Can. J. Microbiol.* **1994**, *40*, 432–438.
- (35) Kier, L. B.; Hall, L. H. *Molecular Connectivity in Structure–Activity Analysis*; Research Studies Press: Chichester, U.K., 1986.
- (36) Sabljic, A.; Horvatic, D. Graph-III—a computer-program for calculating molecular connectivity indexes on microcomputers. *J. Chem. Inf. Comput. Sci.* **1993**, *33*, 292–295.
- (37) Ghose, A. K.; Pritchett, A.; Crippen, G. M. Atomic physicochemical parameters for 3-dimensional structure directed quantitative structure–activity-relationships. 3. Modeling hydrophobic interactions. *J. Comput. Chem.* **1988**, *9*, 80–90.
- (38) Gustafson, K. E.; Dickhut, R. M. Molecular diffusivity of polycyclic aromatic hydrocarbons in aqueous solution. *J. Chem. Eng. Data* **1994**, *39*, 281–285.
- (39) Wammer, K. H. Ph.D. Thesis, Princeton University, Princeton, NJ, 2003.
- (40) van Aarssen, B. G. K.; Bastow, T. P.; Alexander, R.; Kagi, R. I. Distributions of methylated naphthalenes in crude oils: Indicators of maturity, biodegradation and mixing. *Org. Geochem.* **1999**, *30*, 1213–1227.
- (41) Shim, H.; Yang, S. T. Biodegradation of benzene, toluene, ethylbenzene, and *o*-xylene by a coculture of *Pseudomonas putida* and *Pseudomonas fluorescens* immobilized in a fibrous-bed bioreactor. *J. Biotechnol.* **1999**, *67*, 99–112.
- (42) Bielefeldt, A. R.; Stensel, H. D. Evaluation of biodegradation kinetic testing methods and longterm variability in biokinetics for BTEX metabolism. *Water Res.* **1999**, *33*, 733–740.
- (43) Goudar, C. T.; Strevett, K. A. Comparison of relative rates of BTEX biodegradation using respirometry. *J. Ind. Microbiol. Biotechnol.* **1998**, *21*, 11–18.
- (44) Duetz, W. A.; Wind, B.; van Andel, J. G.; Barnes, M. R.; Williams, P. A.; Rutgers, M. Biodegradation kinetics of toluene, *m*-xylene, *p*-xylene and their intermediates through the upper TOL pathway in *Pseudomonas putida* (PWW0). *Microbiology-Sgm* **1998**, *144*, 1669–1675.
- (45) Parsons, J. R.; Govers, H. A. J. Quantitative structure–activity relationships for biodegradation. *Ecotoxicol. Environ. Saf.* **1990**, *19*, 212–227.
- (46) Bugg, T.; Foght, J. M.; Pickard, M. A.; Gray, M. R. Uptake and active efflux of polycyclic aromatic hydrocarbons by *Pseudomonas fluorescens* LP6a. *Appl. Environ. Microbiol.* **2000**, *66*, 5387–5392.
- (47) Gibson, D. T.; Parales, R. E. Aromatic hydrocarbon dioxygenases in environmental biotechnology. *Curr. Opin. Biotechnol.* **2000**, *11*, 236–243.

*Received for review July 9, 2004. Revised manuscript received January 18, 2005. Accepted January 26, 2005.*

ES048939Y